

B.E. GRINYUK, D.V. PIATNYTSKYI

Bogolyubov Institute for Theoretical Physics, Nat. Acad. of Sci. of Ukraine

(14b, Metrolohichna Str., Kyiv 03680, Ukraine; e-mail: bgrinyuk@bitp.kiev.ua, dumpyat@gmail.com)

## STRUCTURE OF $^{14}\text{C}$ AND $^{14}\text{O}$ NUCLEI CALCULATED IN THE VARIATIONAL APPROACH

UDC 539.172

*The structure of mirror  $^{14}\text{C}$  and  $^{14}\text{O}$  nuclei has been studied in the framework of the five-particle model (three  $\alpha$ -particles and two nucleons). Interaction potentials are proposed, which allowed the energy and radius of  $^{14}\text{C}$  nucleus, as well as the energy of  $^{14}\text{O}$  one, to agree with experimental data. On the basis of the variational approach with the use of Gaussian bases, the energies and wave functions for five-particle systems under consideration are calculated. The charge radius of  $^{14}\text{O}$  nucleus, as well as the charge density distributions and the form factors for both nuclei, are predicted.*

*Keywords:* root-mean-square radius, density distribution, charge form factor,  $^{14}\text{C}$  nucleus,  $^{14}\text{O}$  nucleus.

### 1. Introduction

Each of the radioactive  $^{14}\text{C}$  and  $^{14}\text{O}$  nuclei can be imagined as composed of three  $\alpha$ -particles and two extra nucleons. The experience of the theoretical researches of nuclei with two extra nucleons such as  $^6\text{He}$  and  $^6\text{Li}$  [1–3] or more complicated  $^{10}\text{Be}$  and  $^{10}\text{C}$  ones [4, 5] showed that the accuracy of this approximation can compete with that of other approaches, in which all nucleon degrees of freedom are taken into consideration [6]. If the number of nucleons in a nucleus is large, the reduction of the number of variables in the corresponding problem by making allowance for the  $\alpha$ -clustering becomes even more justified.

In this work, we consider  $^{14}\text{C}$  and  $^{14}\text{O}$  nuclei as systems consisting of three  $\alpha$ -particles and two extra neutrons (in  $^{14}\text{C}$  case) or two extra protons (for  $^{14}\text{O}$  nucleus). The problem of five particles is solved in the variational approach with the use of the Gaussian basis [7–9], which allows the systems of several particles with various kinds of interaction between them to be studied with a rather high accuracy.

The applied models of generalized interaction potentials between  $\alpha$ -particles, as well as between nucleons and  $\alpha$ -particles, are similar to those used by us in the research of lighter nuclei [3, 5, 10]. However, for the agreement of the energy and charge radius of  $^{14}\text{C}$  nucleus and the energy of  $^{14}\text{O}$  nucleus with experimental values to be exact, the parameters of potentials are slightly modified. This gives us a ground to hope for that the density distributions and charge form factors predicted for  $^{14}\text{C}$  and  $^{14}\text{O}$  nuclei – in particular, the charge radius of  $^{14}\text{O}$  – will agree with future experimental data.

### 2. Statement of the Problem

The model Hamiltonian for  $^{14}\text{O}$  nucleus contains, besides the one-particle operator of kinetic energy, the potentials of pair interaction between the particles, which are generated by nuclear forces, and the Coulomb repulsion potential,

$$\hat{H} = \sum_{i=1}^2 \frac{\mathbf{p}_i^2}{2m_p} + \sum_{i=3}^5 \frac{\mathbf{p}_i^2}{2m_\alpha} + U_{pp}(r_{12}) + \sum_{j>i=3}^5 \hat{U}_{\alpha\alpha}(r_{ij}) + \sum_{i=1}^2 \sum_{j=3}^5 \hat{U}_{p\alpha}(r_{ij}) + \sum_{j>i=1}^5 \frac{Z_i Z_j e^2}{r_{ij}}. \quad (1)$$

Here,  $m_p$  and  $m_\alpha$  are the masses of a proton and an  $\alpha$ -particle, respectively;  $Z_1 = Z_2 = 1$  and  $Z_3 = Z_4 = Z_5 = 2$  are the charges of particles divided by the elementary charge unit  $e$ . Note that the Hamiltonian for  $^{14}\text{C}$  nucleus differs from Eq. (1) in that the neutron charges equal zero ( $Z_1 = Z_2 = 0$ ) and the proton mass  $m_p$  is substituted by the neutron one  $m_n$ , although this change of mass practically does not affect the result. The Hamiltonians for both nuclei are also characterized by a small difference between the effective nuclear interaction of a neutron with an  $\alpha$ -particle in  $^{14}\text{C}$  nucleus and the effective interaction of a proton with an  $\alpha$ -particle in  $^{14}\text{O}$  one, because the distribution of protons in the  $\alpha$ -particle has a little larger radius than the corresponding distribution of neutrons (see, e.g., work [11]).

The choice of models for the pair interaction potentials between the particles is based on the criterion that our model should simultaneously describe the experimental energies of the examined nuclei and the charge radius of  $^{14}\text{C}$  nucleus (the experimental charge radius for  $^{14}\text{O}$  is unknown). The pair interaction potential between the neutrons in  $^{14}\text{C}$  nucleus is chosen in the form of a local potential that describes both the low-energy singlet neutron-neutron parameters and the singlet phase of the neutron scattering with a qualitative accuracy. In view of the charge invariance of nuclear forces, the interaction potential between the protons in  $^{14}\text{O}$  nucleus,  $U_{pp}(r)$ , is assumed to be the same. This potential was successfully used, while studying  $^6\text{He}$  [3],  $^{10}\text{Be}$ , and  $^{10}\text{C}$  [5, 10] nuclei.

The interaction potential between a neutron and an  $\alpha$ -particle is chosen in the form of a generalized interaction potential with the local and nonlocal components, which models most successfully the interaction of a nucleon with the  $\alpha$ -cluster [1, 3] and simulates the Pauli exclusion principle. In work [5], in order to study  $^{10}\text{Be}$  nucleus, the parameters of the potential between a neutron and an  $\alpha$ -particle that had been used to study  $^6\text{He}$  nucleus [3] were slightly changed. In the present work, analogously to this procedure, some parameters of the same potential are changed a little in order to simultaneously describe the energy and charge radius of  $^{14}\text{C}$  with a high accuracy:

$$\hat{U}_{n\alpha}(r) = -V_0 \exp(-(r/r_0)^2) + \frac{g}{\pi^{3/2}R_0^3}|u\rangle\langle u|, \quad (2)$$

where the local attraction is characterized by the parameters  $V_0 = 43.95$  MeV and  $r_0 = 2.25$  fm, and the separable repulsion has the form factor  $u(r) = \exp(-(r/R_0)^2)$  with the radius  $R_0 = 2.79$  fm and the repulsion intensity  $g = 140\lambda(R_0)$  MeV (hereafter,  $\lambda(x) \equiv [2/(\pi x^2)]^{3/2}$ ).

The interaction potential between a proton and an  $\alpha$ -particle that was used by us to study  $^{14}\text{O}$  nucleus had the same form (2), but with slightly changed parameters. This circumstance is related to the known fact that the protons and neutrons in  $^4\text{He}$  nucleus are not distributed absolutely identically (the details of distributions can be found in work [11]), so that the potential of nuclear interaction  $\hat{U}_{n\alpha}$  should not exactly coincide with the potential  $\hat{U}_{p\alpha}$ . We select the parameters for the potential  $\hat{U}_{p\alpha}$  so that the energy of  $^{14}\text{O}$  nucleus could be described by assuming the other potentials of nuclear interaction between the corresponding particles in  $^{14}\text{O}$  and  $^{14}\text{C}$  nuclei to be identical. In this work, the attraction intensity  $V_0 = 44.757$  MeV and the attraction radius  $r_0 = 2.27$  fm are used for the potential  $\hat{U}_{p\alpha}$ . The separable repulsion component of this potential is taken the same as for the potential  $\hat{U}_{n\alpha}$  (2).

By its form, the interaction potential between  $\alpha$ -particles is also very similar to that used in work [5]: it has local and nonlocal components, but with slightly modified parameters:

$$\hat{U}(r) = -U_1 \exp(-(r/\rho_1)^2) + U_2 \exp(-(r/\rho_2)^2) + \frac{g}{\pi^{3/2}\rho_\alpha^3}|v\rangle\langle v|, \quad (3)$$

where the attraction intensity  $U_1 = 43.5$  MeV, the repulsion intensity  $U_2 = 240.0$  MeV, and the corresponding radii equal  $\rho_1 = 2.55$  fm and  $\rho_2 = 1.3$  fm, respectively. The separable repulsion has the form factor  $v(r) = \exp(-(r/\rho_\alpha)^2)$  with the radius  $\rho_\alpha = 1.765$  fm, and the repulsion intensity  $g = 60\lambda(\rho_\alpha)$  MeV.

Note that the selection of parameters for the potentials became possible only after a multiply repeated procedure that includes the solution of the five-particle problem and the comparison of the values obtained for the energy and the charge radius with the experimental data. The method of calculation on

the basis of the variational approach with the use of Gaussian bases will be briefly described in the next section. The resulting potential parameters are given above, and the energies and radii calculated on the basis of those potentials for both analyzed nuclei are compared with the corresponding experimental data in Table 1. In the latter, the energies of nuclei are shown subtracting  $-28.296$  MeV per each  $\alpha$ -particle, and the charge radii were calculated with regard for the non-point character of the particles in the Helm approximation:

$$R_{\text{ch}}^2 = R_{\alpha}^2 + R_{\text{ch}}^2(^4\text{He})$$

in the case of  $^{14}\text{C}$  nucleus (a small squared charge radius of a neutron is neglected) and

$$R_{\text{ch}}^2 = \frac{3}{4} (R_{\alpha}^2 + R_{\text{ch}}^2(^4\text{He})) + \frac{1}{4} (R_p^2 + R_{\text{ch}}^2(p))$$

for  $^{14}\text{O}$  one. Here,  $R_{\alpha}$  designates the root-mean-square radius for “point-like”  $\alpha$ -particles distribution, which was calculated in the framework of the model with Hamiltonian (1), and the charge radius of  $\alpha$ -particle  $R_{\text{ch}}(^4\text{He}) = 1.679$  fm was taken from the experiment (as an average value between the modern data [12] and the data of work [13]). Analogously,  $R_p$  means the calculated root-mean-square radius of the “point-like” proton distribution (in the case of  $^{14}\text{O}$  nucleus), and  $R_{\text{ch}}(p) = 0.875$  fm was taken from the experimental data of work [14].

### 3. Calculation Technique

To solve the problem of bound states in the system of five particles, we use the variational method in the Gaussian representation [7–9], which allows the wave function of the system to be obtained in the explicit convenient form of a gaussoid superposition. Omitting the details of this well-known method,

**Table 1. Energies (MeV) and charge radii (fm) of  $^{14}\text{C}$  and  $^{14}\text{O}$  nuclei. The energies are reckoned from the threshold of the nucleus decay into three  $\alpha$ -particles and two nucleons**

Nucleus	$E$	$E_{\text{exp}}$	$R_{\text{ch}}$	$R_{\text{ch, exp}}$
$^{14}\text{C}$	$-20.398$	$-20.398$	$2.500$	$2.496$ [17] $2.503$ [12]
$^{14}\text{O}$	$-13.845$	$-13.845$	$2.415$	—

we only recall that the Schrödinger equation with Hamiltonian (1) can be reduced to a system of linear algebraic equations (the Galerkin method):

$$\sum_{m=1}^K C_m \langle \hat{S}\varphi_k | \hat{H} - E | \hat{S}\varphi_m \rangle = 0, \quad k = 0, 1, \dots, K. \quad (4)$$

Here, all required matrix elements are expressible in an explicit form if one uses the Gaussian basis. For the ground symmetric  $J^{\pi} = 0^+$  state, the wave function  $\Phi$  has a simple form in the Gaussian representation:

$$\begin{aligned} \Phi &= \hat{S} \sum_{k=1}^K C_k \varphi_k \equiv \\ &\equiv \hat{S} \sum_{k=1}^K C_k \exp\left(-\sum_{j>i=1}^5 a_{k,ij} (\mathbf{r}_i - \mathbf{r}_j)^2\right), \end{aligned} \quad (5)$$

where  $\hat{S}$  is the symmetrizing operator. Note also that the wave function symmetrization can be either performed or not performed explicitly, because, as was shown in work [15], the symmetric form is restored automatically, when the non-symmetrized basis is expanded. Both opportunities are used in this work. The explicit symmetrizations for three  $\alpha$ -particles and two extra nucleons (in this case, there are only  $3! \times 2 = 12$  terms in the symmetrized function) allowed a Gaussian basis with considerably smaller dimensionality to be used than that required in the case of the wave function with no explicit symmetrization, provided the same calculation accuracy.

### 4. Density Distributions and Form Factors

The one-particle density distribution for the  $j$ -th particle in a system of particles with the wave function  $|\Phi\rangle$  is defined as follows:

$$n_i(r) = \langle \Phi | \delta(\mathbf{r} - (\mathbf{r}_i - \mathbf{R}_{\text{c.m.}})) | \Phi \rangle, \quad (6)$$

where  $\mathbf{R}_{\text{c.m.}}$  is the radius vector of the center of mass of the system. Hereafter, all density distributions are normalized to 1:  $\int n_i(r) d\mathbf{r} = 1$ . The expressions for

$n_i(r)$  have the explicit form in terms of the parameters  $a_{k,ij}$  and the coefficients  $C_k$  of the linear expansion of the wave function in the Gaussian representation (5). The resulting one-particle density distributions multiplied by  $r^2$  are shown in Fig. 1 by dashed curves. They illustrate the density distributions for “point-like”  $\alpha$ -particles and extra nucleons in  $^{14}\text{C}$  nucleus. The corresponding distributions of “point-like” particles in  $^{14}\text{O}$  nucleus are very similar to those depicted in Fig. 1, so that they are not exhibited separately. The attention is attracted by the fact that the extra nucleons are mainly located inside  $^{12}\text{C}$  cluster formed by  $\alpha$ -particles (with a probability of about 0.86 for neutrons in  $^{14}\text{C}$  nucleus and 0.84 for protons in  $^{14}\text{O}$  nucleus). However, another small maximum in the density distribution curve for extra nucleons testifies that the extra nucleons can also be found outside  $^{12}\text{C}$  cluster, although with rather a low probability (approximately 0.14 for  $^{14}\text{C}$  and 0.16 for  $^{14}\text{O}$ ).

Note that the extra nucleons move much more rapidly than the  $\alpha$ -particles. In particular, the calculated average kinetic energy amounts to about 32.66 MeV for each of the extra neutrons in  $^{14}\text{C}$  nucleus. At the same time, the corresponding value for each  $\alpha$ -particle equals about 6.83 MeV, which is almost five times lower and can be explained, mainly, by the larger mass of the latter. Concerning the particle velocities, it turns out that the extra neutrons in  $^{14}\text{C}$  nucleus move approximately 4.4 times faster than the  $\alpha$ -particles. The same ratio between the velocities of extra nucleons and  $\alpha$ -particles is characteristic of  $^{14}\text{O}$  nucleus. For the latter, the calculated average kinetic energy amounts to about 31.77 MeV for each extra proton and to about 6.62 MeV for each  $\alpha$ -particle.

To calculate the charge density distribution in the nuclei, the non-point nature of  $\alpha$ -particles, as well as protons in the case of  $^{14}\text{O}$  nucleus, has to be taken into consideration. For this purpose, we use the Helm approximation [16]. In particular, the charge density distribution for  $^{14}\text{C}$  nucleus,

$$n_{\text{ch}}(r) = \int n_{\alpha}(|\mathbf{r} - \mathbf{r}'|) n_{\text{ch},^4\text{He}}(r') d\mathbf{r}', \quad (7)$$

looks like the convolution of the one-particle density distribution  $n_{\alpha}$  found for “point-like”  $\alpha$ -particles with the charge density of an  $\alpha$ -particle itself,  $n_{\text{ch},^4\text{He}}$ , which follows from the experimental form factor [18].

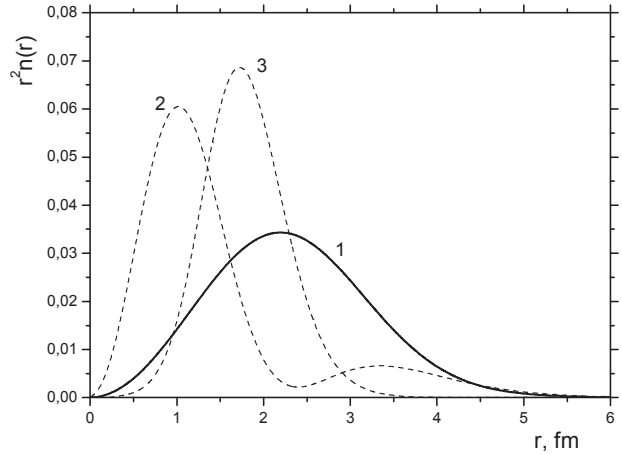


**Fig. 1.** Charge density distribution in  $^{14}\text{C}$  nucleus multiplied by  $r^2$  (solid curve 1). Dashed curves correspond to the density distributions (multiplied by  $r^2$ ) of “point-like” particles: extra neutrons (curve 2) and  $\alpha$ -particles (curve 3)

In expression (7), we neglect a small contribution of extra neutrons to the charge density distribution. Note that the Helm approximation (7) is obtained, by supposing that the wave function of a nucleus is an (approximate) product of the wave function obtained for the Hamiltonian that describes the relative motion of “point-like” particles with the wave functions of  $^4\text{He}$  nuclei ( $\alpha$ -clusters).

A similar expression is obtained for  $^{14}\text{O}$  nucleus, in which, besides the contribution of  $\alpha$ -particles to the density distribution, the contribution of extra protons is also made allowance for:

$$n_{\text{ch}}(r) = \frac{3}{4} \int n_{\alpha}(|\mathbf{r} - \mathbf{r}'|) n_{\text{ch},^4\text{He}}(r') d\mathbf{r}' + \frac{1}{4} \int n_p(|\mathbf{r} - \mathbf{r}'|) n_{\text{ch},p}(r') d\mathbf{r}'. \quad (8)$$

Here, the charge distribution for a proton,  $n_{\text{ch},p}$ , is taken from work [19]. The coefficients 3/4 and 1/4 (their sum equals 1) are proportional to the total charges of  $\alpha$ -particles and extra protons, respectively, in  $^{14}\text{O}$  nucleus.

The distributions of charge density in  $^{14}\text{C}$  and  $^{14}\text{O}$  nuclei obtained on the basis of expressions (7) and (8) are shown in Fig. 2. A considerably higher charge density at short distances in  $^{14}\text{O}$  nucleus is explained by the presence of additional proton charges located at rather small distances in this nucleus. For this reason, the charge radius of  $^{14}\text{O}$  nucleus turns out to be

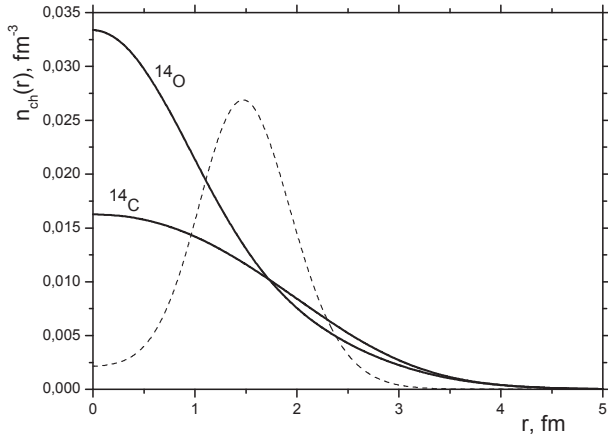


**Fig. 2.** Charge density distributions in  $^{14}\text{C}$  and  $^{14}\text{O}$  nuclei. The dashed curve demonstrates the density distribution for “point-like”  $\alpha$ -particles in  $^{14}\text{C}$  nucleus. The distributions are normalized to 1

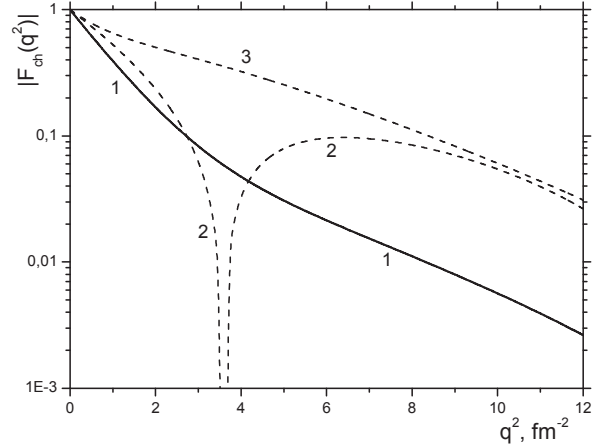


**Fig. 4.** Charge form factor for  $^{14}\text{O}$  nucleus (solid curve 1), form factor corresponding to the density distribution of  $\alpha$ -particles in this nucleus in the “point-like”-particle approximation (curve 2), and analogous form factor obtained for extra protons (curve 3)

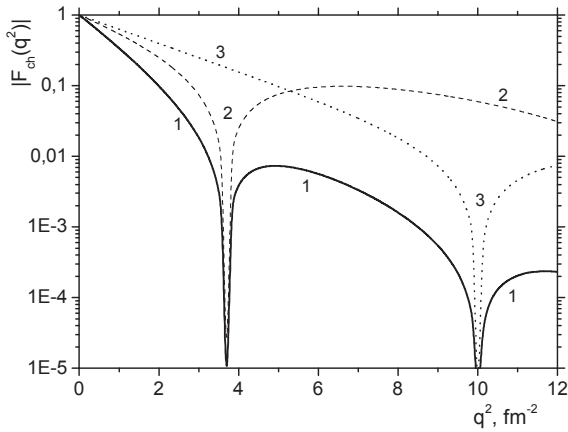


**Fig. 3.** Charge form factor for  $^{14}\text{C}$  nucleus (solid curve 1) in comparison with the same quantity calculated in the “point-like”-particle approximation (dashed curve 2). Curve 3 demonstrates the form factor for  $^4\text{He}$  nucleus [12]

smaller than that of  $^{14}\text{C}$  one:

$$R_{\text{ch}}^2(^{14}\text{O}) = \int r^2 n_{\text{ch},^{14}\text{O}}(r) dr < < R_{\text{ch}}^2(^{14}\text{C}) = \int r^2 n_{\text{ch},^{14}\text{C}}(r) dr, \quad (9)$$

although all distributions for “point-like” particles in  $^{14}\text{O}$  nucleus have, on the contrary, larger radii in comparison with their counterparts in  $^{14}\text{C}$ . This circumstance and a lower binding energy in  $^{14}\text{O}$  nucleus are explained mainly by the additional Coulomb

repulsion due to extra protons. In order to confirm this fact, we quote the calculated root-mean-square relative distances between extra nucleons,  $r_{NN}$ , nucleon and  $\alpha$ -particle,  $r_{N\alpha}$ , and  $\alpha$ -particles,  $r_{\alpha\alpha}$ , as well as the root-mean-square radii for the distributions of “point-like” nucleons,  $R_N$ , and “point-like”  $\alpha$ -particles,  $R_\alpha$ , in both analyzed nuclei in Table 2. We hope for that the value of charge radius  $R_{\text{ch}}(^{14}\text{O}) = 2.415$  fm predicted by us for  $^{14}\text{O}$  nucleus will be experimentally confirmed in the future. With regard for the experimental error for the  $\alpha$ -particle radius [12, 13] and the restricted accuracy of our model, in which the Helm approximation was used, we evaluate the calculation error for the charge radius of  $^{14}\text{O}$  nucleus to equal about  $\pm 0.005$  fm.

Note that the integration (convolution) in Eqs. (7) and (8) substantially “smoothes” out the one-particle distributions obtained for “point-like” particles. As a result, the charge distribution at short distances does not contain a “dip” typical of distributions for “point-like”  $\alpha$ -particles in both nuclei.

**Table 2. Root-mean-square relative distances and radii (fm) of  $^{14}\text{C}$  and  $^{14}\text{O}$  nuclei**

Nucleus	$r_{NN}$	$r_{N\alpha}$	$r_{\alpha\alpha}$	$R_N$	$R_\alpha$	$R_{\text{ch}}$
$^{14}\text{C}$	2.621	2.667	3.189	1.786	1.852	2.500
$^{14}\text{O}$	2.732	2.750	3.239	1.864	1.882	2.415

Characteristic features in the behavior of density distributions manifest themselves in the corresponding form factors, the Fourier transforms of the density. In particular, convolution (7) transforms into the product

$$F_{\text{ch},^{14}\text{C}}(q) = F_{\alpha,^{14}\text{C}}(q) F_{\text{ch},^4\text{He}}(q), \quad (10)$$

and expression (8) into the sum of products

$$F_{\text{ch},^{14}\text{O}}(q) = \frac{3}{4} F_{\alpha,^{14}\text{O}}(q) F_{\text{ch},^4\text{He}}(q) + \frac{1}{4} F_{p,^{14}\text{O}}(q) F_{\text{ch},p}(q). \quad (11)$$

In the products in expressions (10) and (11), the first multipliers correspond to the form factors obtained by us from the wave function of the five-particle problem in the “point-like”-particle approximation. The second multipliers are the experimental form factors of an  $\alpha$ -particle  $F_{\text{ch},^4\text{He}}(q)$  [18] or proton  $F_{\text{ch},p}(q)$  [19]. If a form factor becomes zero at a definite transferred momentum squared, the absolute value of the form factor has a “dip” at this  $q^2$ . Owing to the representation of the charge form factor for  $^{14}\text{C}$  nucleus in the form of product (10), the form factor absolute value has “dips” at those  $q^2$ , where each of the multipliers has its own “dip”, which is illustrated in Fig. 3. Note that the “dip” located at the squared transferred momentum  $q^2 \simeq 10 \text{ fm}^{-2}$  and originating from the form factor of an  $\alpha$ -particle is also observed in the form factors of  $^6\text{He}$  [3] and  $^{10}\text{Be}$  [5] nuclei, as well as in all other cases where the charge distribution in cluster nuclei is driven only by the charges of  $\alpha$ -particles. Concerning the first dip in the charge form factor of  $^{14}\text{C}$  nucleus in the interval slightly below  $q^2 \sim 4 \text{ fm}^{-2}$ , which is connected with the “dip” in the first multiplier in Eq. (10), it is explained by a substantial decrease in the density distribution at short distances, which was obtained in the approximation of “point-like”  $\alpha$ -particles (in Fig. 2, this distribution is depicted by a dashed curve). It can be shown that, after the Fourier transformation, this distribution transforms into a form factor that changes its sign in the momentum representation, and the absolute value of the form factor has a “dip”.

At the same time, in the case of  $^{14}\text{O}$  nucleus, owing to the second term in Eq. (11), the corresponding “dips” do not manifest themselves *per se* in the charge form factor of the nucleus, but only slightly affect

the change of regimes in its behavior, as is shown in Fig. 4. Hence, the form factors of  $^{14}\text{O}$  and  $^{14}\text{C}$  nuclei considerably differ from each other owing to the role of extra protons in  $^{14}\text{O}$  instead of neutrons in  $^{14}\text{C}$ .

## 5. Conclusions

In the framework of the five-particle model (three  $\alpha$ -particles and two extra nucleons) and on the basis of variational calculations in the Gaussian representation, the density distributions and the form factors for  $^{14}\text{C}$  and  $^{14}\text{O}$  nuclei are calculated. The extra nucleons in both nuclei are found to move predominantly inside  $^{12}\text{C}$  cluster, although they can also be found at its periphery with a low probability. The charge radius of  $^{14}\text{O}$  nucleus is predicted. It is shown that, owing to the extra protons that are located closer to the nucleus center, this radius is smaller than that of  $^{14}\text{C}$  nucleus, despite that all relative distances between the corresponding particles in  $^{14}\text{O}$  nucleus are larger than in  $^{14}\text{C}$  one. We hope for that the more detailed ideas of the structure of  $^{14}\text{C}$  and  $^{14}\text{O}$  nuclei and the character of motion of their component particles can be obtained on the basis of calculations and the analysis of such structural functions as the pair correlation functions and the momentum distributions.

1. V.I. Kukulin, V.N. Pomerantsev, Kh.D. Razikov *et al.*, Nucl. Phys. **A 586**, 151 (1995).
2. M.V. Zhukov, B.V. Danilin, D.V. Fedorov *et al.*, Phys. Rep. **231**, 151 (1993).
3. B.E. Grinyuk and I.V. Simenog, Yad. Fiz. **72**,10 (2009).
4. Y. Ogawa, K. Arai, Y. Suzuki, and K. Varga, Nucl. Phys. A **673**, 122 (2000).
5. B.E. Grinyuk and I.V. Simenog, Yad. Fiz. **77**, 443 (2014).
6. A.V. Nesterov, F. Ariks, Ya. Brukkhov, and V.S. Vasilevskii, Elem. Chast. At. Yadro **41**, 1337 (2010).
7. V.I. Kukulin and V.M. Krasnopol'sky, J. Phys. G **3**, 795 (1977).
8. N.N. Kolesnikov and V.I. Tarasov, Yad. Fiz. **35**, 609 (1982).
9. Y. Varga and K. Suzuki, *Stochastic Variational Approach to Quantum-Mechanical Few-Body Problems* (Springer, Berlin, 1998).
10. B.E. Grinyuk and I.V. Simenog, Ukr. J. Phys. **56**, 635 (2011).
11. B.E. Grinyuk, D.V. Piatnytskyi, and I.V. Simenog, Ukr. J. Phys. **52**, 424 (2007).
12. I. Angeli and K.P. Marinova, At. Data Nucl. Data Tables **99**, 69 (2013).
13. I. Sick, Phys. Rev. C **77**, 041302 (2008).

14. *Review of Particle Physics*, J. Phys. G **33**, 1–1232 (2006).
15. I.V. Simenog, M.V. Kuzmenko, and V.M. Khryapa, Ukr. Fiz. Zh. **55**, 1240 (2010).
16. A.I. Akhiezer and V.B. Berestetskii, *Quantum Electrodynamics* (Interscience, New York, 1965).
17. L.A. Schaller, L. Schellenberg, T.Q. Phan *et al.*, Nucl. Phys. **A 379**, 523 (1982).
18. R.F. Frosch, J.S. McCarthy, R.E. Rand, and M.R. Yearian, Phys. Rev. **160**, 874 (1967).
19. P.E. Bosted *et al.*, Phys. Rev. Lett. **68**, 3841 (1992).

Received 17.03.16.

Translated from Ukrainian by O.I. Voitenko

Б.Є. Гринюк, Д.В. П'ятницький

СТРУКТУРА ЯДЕР  $^{14}\text{C}$  ТА  $^{14}\text{O}$   
У ВАРІАЦІЙНОМУ ПІДХОДІ

Резюме

В рамках п'ятичастинкової моделі (три  $\alpha$ -частинки і два додаткові нуклони) досліджено структуру дзеркальних ядер  $^{14}\text{C}$  та  $^{14}\text{O}$ . Запропоновано потенціали взаємодії, які дозволили узгодити з експериментом енергію та радіус ядра  $^{14}\text{C}$ , а також енергію ядра  $^{14}\text{O}$ . На основі варіаційного підходу з використанням гаусоїдних базисів розраховано енергії і хвильові функції досліджуваних п'ятичастинкових систем. Передбачено зарядовий радіус ядра  $^{14}\text{O}$ , а також зарядові розподіли густини і формфактори обох ядер.